J Mater Sci (2009) 44:2466–2470
DOI 10.1007/s10853-009-3314-1

Microstructure, electrical properties of CeO_2-doped $(K_{0.5}Na_{0.5})NbO_3$ lead-free piezoelectric ceramics

Daojiang Gao · K. W. Kwok · Dunmin Lin · H. L. W. Chan

Received: 3 October 2008 / Accepted: 2 February 2009 / Published online: 5 March 2009

Abstract CeO_2-doped $K_{0.5}Na_{0.5}NbO_3$ lead-free piezoelectric ceramics have been fabricated by a conventional ceramic fabrication technique. The ceramics retain the orthorhombic perovskite structure at low doping levels (<1 mol.%). Our results also demonstrate that the Ce-doping can suppress the grain growth, promote the densification, decrease the ferroelectric–paraelectric phase transition temperature (T_C), and improve the dielectric and piezoelectric properties. For the ceramic doped with 0.75 mol.% CeO_2, the dielectric and piezoelectric properties become optimum: piezoelectric coefficient $d_{33} = 130$ pC/N, planar electromechanical coupling coefficient $k_p = 0.38$, relative permittivity $\varepsilon_r = 820$, and loss tangent $\tan\delta = 3\%$.

Introduction

Because of the superior electrical properties, lead zirconate titanate (PZT)-based piezoelectric ceramics have been widely used in actuators, sensors, as well as microelectronic devices. However, as lead is highly toxic, there is a rising concern about manufacture as well as disposal of products containing lead. Therefore, lead-free piezoelectric ceramics, such as $Bi_{0.5}Na_{0.5}TiO_3$ (BNT)-based ceramics [1, 2], bismuth-layered structure ceramics [3, 4], tungsten bronze-type ceramics [5], $BaTiO_3$-based ceramics [6], and alkaline niobate-based ceramics [7, 8] have recently been studied extensively for replacing the lead-containing materials in various applications. Among various lead-free candidates, $K_{0.5}Na_{0.5}NbO_3$ (KNN) has been considered one of the most promising alternatives because of its high Curie temperature and good ferroelectric and piezoelectric properties. However, it is very difficult to obtain dense and well-sintered KNN ceramics using an ordinary sintering process because of the high volatility of alkaline elements at high temperatures. A number of studies have been carried out to improve the sintering performance and then the piezoelectric properties of KNN ceramics; these include the formation of solid solutions of KNN with other ferroelectrics or non-ferroelectrics, e.g., KNN–$SrTiO_3$ [7] and KNN–$LiTaO_3$ [9], and the use of sintering aids, e.g., $K_4CuNb_8O_{23}$ [10], MnO_2 [11], CuO [12], and Bi_2O_3 [8].

CeO_2 is often used as a donor dopant or additive for the lead-based piezoelectric ceramics [13–15] to improve their electrical properties. Recently, it has also been used for the BNT-based [16, 17] and $BaTiO_3$-based [18] lead-free piezoelectric ceramics, and promising results have been obtained. However, there is little work reporting on the CeO_2-doping in KNN-based ceramics. Zuo et al. have studied the effects of CeO_2 on the microstructure and densification of KNN ceramic; however, the resulting effects on the piezoelectric properties have not been reported [19]. In the present work, $K_{0.5}Na_{0.5}NbO_3$ ceramics doped with CeO_2 were prepared by an ordinary sintering technique, and the resulting effects on the structure, dielectric, ferroelectric, and piezoelectric properties were investigated.

Experimental

A conventional ceramic fabrication technique was used to prepare $K_{0.5}Na_{0.5}NbO_3 + x$ mol.% CeO_2 (abbreviated as

D. Gao (✉) · K. W. Kwok · D. Lin · H. L. W. Chan
Department of Applied Physics and Materials Research Centre, The Hong Kong Polytechnic University, Kowloon, Hong Kong, China
e-mail: daojianggao@126.com

KNN–Ce-x) ceramics. Analytical-grade metal oxides or carbonate powders: K_2CO_3 (99.9%), Na_2CO_3 (99.5%), Nb_2O_5 (99.95%), and CeO_2 (99.99%) were used as raw materials. The powders in the stoichiometric ratio of $K_{0.5}Na_{0.5}NbO_3$ were mixed thoroughly in ethanol using zirconia balls for 8 h, and then dried and calcined at 880 °C for 6 h. After the calcination, CeO_2 was added. The resulting mixture was ball-milled again for 8 h and mixed thoroughly with a PVA binder solution, and then pressed into disk samples with a diameter of 15 mm and a thickness of 1 mm. The disk samples were finally sintered at 1,100–1,180 °C for 4 h in air. Silver electrodes were fired on the top and bottom surfaces of the samples. The ceramics were poled under a dc field of 5–6 kV/mm at 180 °C in a silicone oil bath for 30 min.

The crystalline structure of the sintered samples was examined using X-ray diffraction (XRD) analysis with CuK_α radiation (Bruker D8 Discover). The microstructure was observed using a scanning electron microscopy (JEOL, JSM-6490). The density of the samples was measured by the Archimedes method. The relative permittivity ε_r was measured as a function of temperature using an impedance analyzer (HP 4192A). A conventional Sawyer-Tower circuit was used to measure the polarization hysteresis (P–E) loop at 150 Hz. The planar electromechanical coupling coefficient k_p was determined by the resonance method according to the IEEE Standard 176 using an impedance analyzer (HP 4294A). The piezoelectric coefficient d_{33} was measured using a piezo-d_{33} meter (ZJ-3A, China).

Results and Discussion

Figure 1 shows the XRD patterns of the KNN–Ce-x ceramics. All the ceramics possess essentially a single-phase perovskite structure, suggesting that CeO_2 has diffused into the lattices of KNN to form a solid solution. Ce ions may exist in the KNN structure in two valence states: Ce^{4+} with a radius of 0.92 Å and Ce^{3+} with a radius of 1.03 Å. Both of them are much larger than Nb^{5+} (0.64 Å), but have similar size of Na^+ (1.02 Å) and K^+ (1.33 Å). Therefore, according to the principles of crystal chemistry and radius-matching rule, they enter most likely the A-sites for substituting K^+ or Na^+, and serve as the donor-type dopants for the ceramics. A number of minor peaks were observed in the ranges of 2θ from 25° to 30° and from 35° to 40°, which may be arisen from the secondary phases. However, the peaks are very small (which can only be observed by plotting the intensity in log scale), so the amount of the secondary phase should be very little and hence their effects should be insignificant. As shown in the enlarged XRD patterns of the ceramics in the range of 2θ from 44° to 48° (Fig. 1b), the ceramics with $x \leq 1$ have an orthorhombic perovskite structure. As x increases, the two diffraction peaks (202) and (020) start to merge into a broad single peak gradually, suggesting that the ceramic may have a tendency to transform into another phase, e.g., pseudocubic phase, at high doping levels of CeO_2. Similar results have been reported for the La-modified BNBT [16] and BNT [17]. In general, the doping of CeO_2 will induce a structure phase transformation.

Figure 2 shows the SEM micrographs of the KNN–Ce-x ceramics with $x = 0$, 0.5, 1, and 1.5 sintered at the optimal sintering temperature. For each composition, the ceramics were sintered at different temperatures and their density was measured. The optimum sintering temperature was determined as the sintering temperature by which the ceramic had the largest density. As shown in Fig. 2a, the KNN ceramic (i.e., with $x = 0$) is well crystallized and the grains are large, with a diameter of ~10 μm. After the

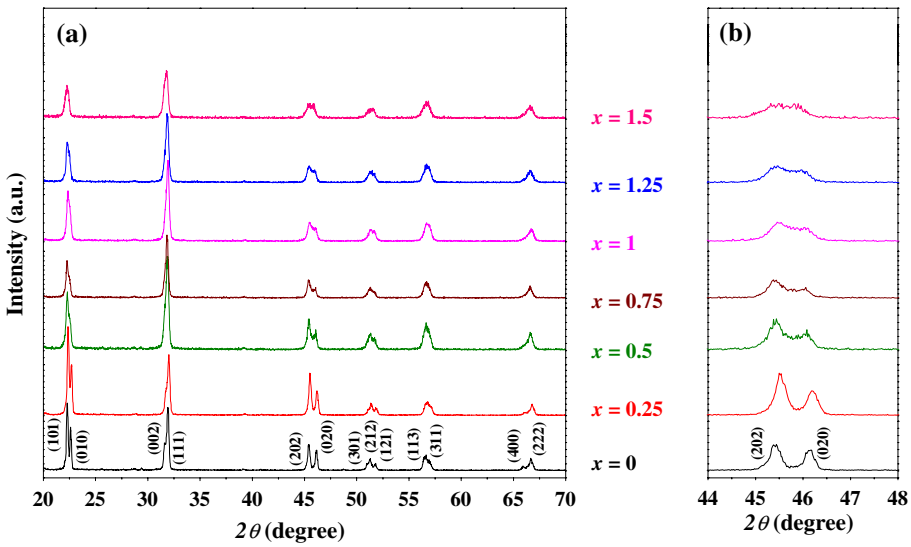

Fig. 1 X-ray diffraction patterns of the KNN–Ce-x ceramics in the range of 2θ **a** from 20° to 70° and **b** from 44° to 48°

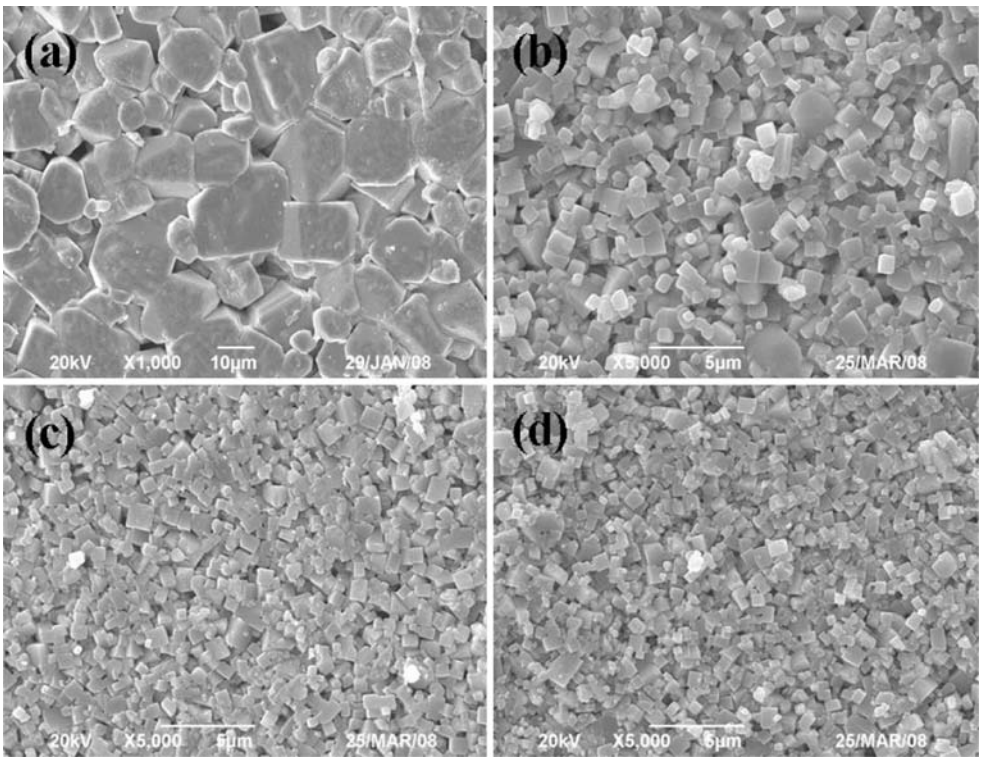

Fig. 2 SEM micrographs of the KNN–Ce-x ceramics sintered at the optimal sintering temperature: **a** $x = 0$, sintered at 1,100 °C for 4 h; **b** $x = 0.5$, sintered at 1,170 °C for 4 h; **c** $x = 1.0$, sintered at 1,170 °C for 4 h; **d** $x = 1.5$, sintered at 1,175 °C for 4 h

doping of a small amount of CeO_2 ($x = 0.5$), the grain size decreases significantly to about 2 μm (Fig. 2b). The grain size continues to decrease with increasing x. For the ceramic with $x = 1.5$, the grain size is about 0.5 μm (Fig. 2d). It can also be seen that the optimum sintering temperature is increased after the doping of CeO_2, from about 1,100 °C to 1,170–1,180 °C. In general, the grains will grow larger at a higher sintering temperature. Therefore, our results (the decrease in the grain size) clearly show that CeO_2 is effective in suppressing the melting and grain growth of the KNN ceramics during sintering. This should be attributed to the donor-type nature of Ce. For PZT-based ceramics, donor doping generally causes an inhibition of grain growth [20, 21]. The sintering kinetics can be described by the lattice diffusion of vacancies from pores to grain boundaries, and the donor doping reduces the diffusion coefficient: the vacancies (e.g., A-site vacancies in our case) created by the doping are supposed to be bound to the impurity ion (e.g., Ce^{3+} in our case). As a result, the mass transportation is weakened and the grain growth is inhibited.

Figure 3 shows the variations of the density and relative density (to the theoretical density of KNN, 4.51 g/cm^3) with x (the doping level of CeO_2) for the KNN–Ce-x ceramics sintered at the optimal sintering temperature. The observed density and relative density increase with increasing x and then decrease, giving a maximum value of 4.379 g/cm^3 and

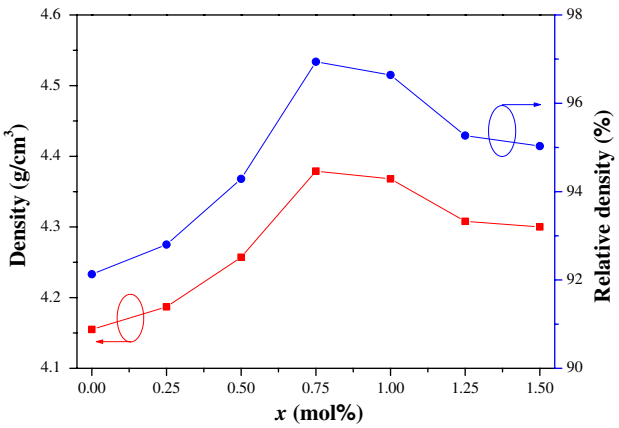

Fig. 3 Variations of the density and relative density with x for the KNN–Ce-x ceramics sintered at the optimal sintering temperature

96.94%, respectively, at $x = 0.75$. It is also seen that all the Ce-doped KNN ceramics have a higher density than the KNN ceramic. This clearly shows that the doping of CeO_2 is effective in promoting the densification of the ceramics.

Figure 4 shows the temperature dependences of the relative permittivity ε_r (measured at 10 kHz) for the KNN–Ce-x ceramics with $x = 0$, 0.5, 1, and 1.5. The KNN–Ce-0 (i.e., KNN) ceramic undergoes two phase transitions: the paraelectric cubic–ferroelectric tetragonal phase transition

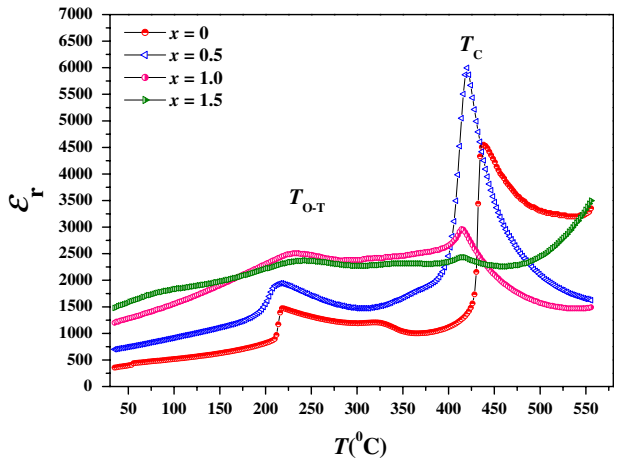

Fig. 4 Relative permittivity ε_r (measured at 10 kHz) as a function of temperature for the KNN–Ce-x ceramics with $x = 0$, 0.5, 1.0, and 1.5, respectively

at 438 °C (T_C) and the ferroelectric tetragonal–ferroelectric orthorhombic phase transition at 218 °C (T_{O-T}). After the doping of CeO_2, the ceramics exhibit similar phase transitions at different T_C and T_{O-T}. In general, the observed T_C decreases slightly from 438 to 416 °C at a rate of ~14 °C/1 mol.% as x increases from 0 to 1.5, while T_{O-T} increases slightly from 218 to 243 °C. Similar results have been reported for the CeO_2-doped PZT [15], PMN-PT [13], and BNKT ceramics [22]. It is also noted that, at high doping levels of Ce, in particular for $x = 1.5$, the two phase transition peaks become weakened and broadened. This may be attributed to the structure transformation of the ceramics (Fig. 1).

All the ceramics exhibit a typical P–E loop. Figure 5 shows, as examples, the P–E loops of the KNN–Ce-x ceramics with $x = 0$, 0.5, 1.0, and 1.25. It can be seen that the P–E loop for the KNN–Ce-0 ceramic is square-like, showing a large remanent polarization ($P_r = 21.0$ μC/cm^2) and a small coercive field ($E_c = 1.2$ kV/mm). After the doping of CeO_2, the P–E loop becomes slanted (Fig. 5). At $x = 0.5$, the observed P_r remains unchanged while E_c decreases to 0.93 kV/mm. As x increases, P_r starts to decrease significantly, giving a value of 17.5 and 13.2 μC/cm^2 at $x = 1.0$ and 1.25, respectively. Unlike P_r, the observed E_c remains almost unchanged as x increases from 0.5 to 1.25. It should be noted that a well-saturated P–E loop cannot be obtained for the KNN–Ce-1.5 ceramic because of the large leakage current.

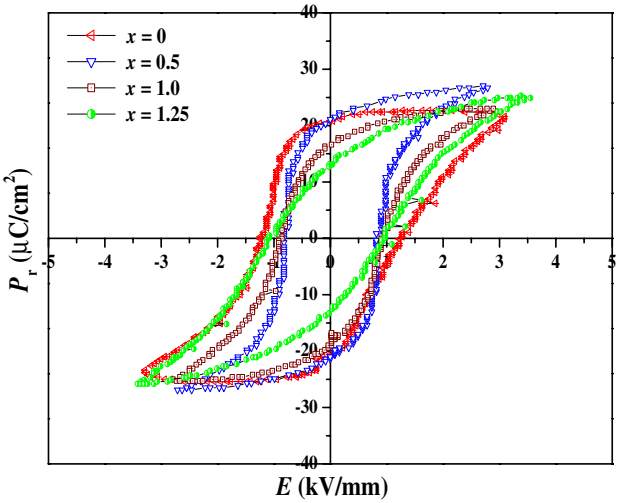

Fig. 5 P–E hysteresis loops of the KNN–Ce-x ceramics with $x = 0$, 0.5, 1.0, and 1.25

The variations of d_{33}, k_P, ε_r, and tanδ with x for the KNN–Ce-x ceramics are shown in Fig. 6. Both the observed d_{33} and k_p increase with increasing x and then decrease, giving a maximum value of 130 pC/N and 0.38, respectively, at $x = 0.75$ (Fig. 6a). Unlike d_{33} and k_p, ε_r increases continuously with increasing x (Fig. 6b). This may be attributed to the presence of the donor cations in the lattices. On the other hand, the loss tangent tanδ decreases with increasing x and increase, having a small value of 3% at $x = 0.75$. The largest d_{33} and k_p value of the KNN–Ce-0.75 ceramic may also be attributed to the highest density (Fig. 3) and the lowest loss tangent tanδ.

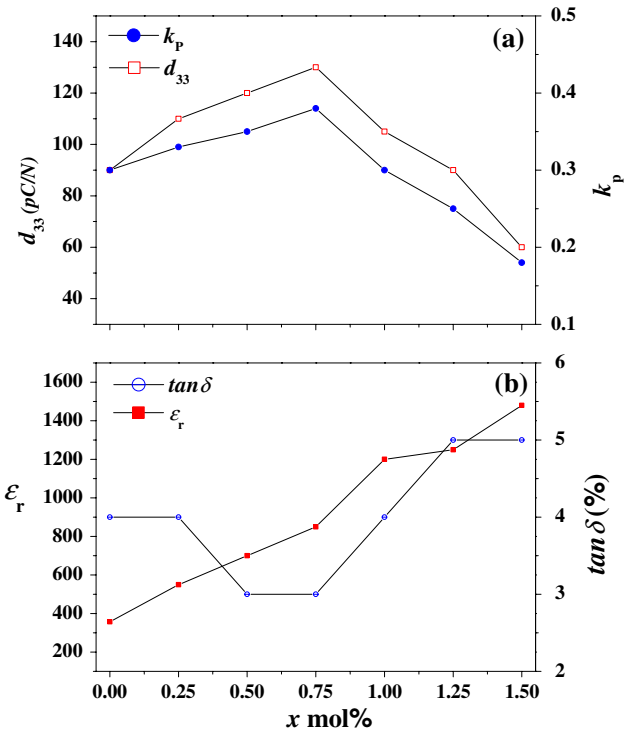

Fig. 6 **a** Variations of the piezoelectric coefficient d_{33} and planar electromechanical coupling coefficient k_p with x for the KNN–Ce-x ceramics and **b** variations of the relative permittivity ε_r and loss tangent tanδ with x for the KNN–Ce-x ceramics

Conclusions

KNN–Ce-x lead-free piezoelectric ceramics have been fabricated by a conventional ceramic fabrication technique. At $x \leq 1$, the ceramic exhibits a single-phase perovskite structure with orthorhombic symmetry. Our results also show that the Ce-doping can suppress the grain growth, promote the densification, decrease the ferroelectric–paraelectric phase transition temperature (T_C), and improve the dielectric and piezoelectric properties. For the KNN–Ce-0.75 ceramic, the dielectric and piezoelectric properties become optimum: piezoelectric coefficient $d_{33} = 130$ pC/N, planar electromechanical coupling coefficient $k_p = 0.38$, relative permittivity $\varepsilon_r = 820$, and loss tangent $\tan\delta = 3\%$.

Acknowledgements This work was supported by the Research Grants Council of the Hong Kong Special Administrative Region (Project No. PolyU 5188/06E) and the Centre for Smart Materials of The Hong Kong Polytechnic University.

References

1. Lin DM, Xiao DQ, Zhu JG, Yu P (2006) Appl Phys Lett 88: 062901
2. Takenaka T, Maruyama K, Sakata K (1991) Jpn J Appl Phys 30: 2236
3. Wang CM, Wang JF, Gai ZG (2007) Script Mater 57:789
4. Jardiel T, Caballero AC, Villegas M (2007) J Eur Ceram Soc 27:4115
5. Xie RJ, Akimune Y, Matsuo K, Sugiyama T (2002) Appl Phys Lett 80:835
6. Yu Z, Ang C, Guo R, Bhalla AS (2002) J Appl Phys 92:1489
7. Guo YP, Kakimoto K, Ohsato H (2004) Solid State Commun 129:279
8. Du HL, Luo F, Qu SB, Pei ZB, Zhu DM, Zhou WC (2007) J Appl Phys 102:054102
9. Guo YP, Kakimoto K, Ohsato H (2005) Mater Lett 59:241
10. Matsubara M, Yamaguchi T, Kikuta K, Hirano S (2004) Jpn J Appl Phys 43:7159
11. Lin DM, Kwok KW, Tian HY, Chan HLW (2007) J Am Ceram Soc 90:1458
12. Lin DM, Kwok KW, Chan HLW (2007) Appl Phys Lett 90: 232903
13. Sahoo B, Panda PK (2007) J Mater Sci 42:4745. doi:10.1007/s10853-006-0828-7
14. Srimaungsong P, Udomkan N, Pdungsap L, Winotai P (2005) Int J Mod Phys B 19:1757
15. Jin D, Hing P, Sun CQ (2000) J Phys D Appl Phys 33:744
16. Wang XX, Chan HLW, Choy CL (2005) Appl Phys A 80:333
17. Herabut A, Safari A (1997) J Am Ceram Soc 80:2954
18. Aparna M, Bhimasankaram T, Suryanarayana SV, Prasad G, Umar GSK (2001) Bull Mater Sci 24:497
19. Zuo RZ, Rödel J, Chen RZ, Li LT (2006) J Am Ceram Soc 89:2010
20. Lee BW, Lee EJ (2006) J Electroceram 17:597
21. Pereira M, Peixoto AG, Gomes MJM (2001) J Eur Ceram Soc 21:1353
22. Li YM, Chen W, Xu Q, Zhou J, Wang Y, Sun HJ (2007) Ceram Int 33:95